

Interference pattern generation in evanescent electromagnetic waves for nanoscale lithography using waveguide diffraction gratings

E.A. Bezus, L.L. Doskolovich, N.L. Kazanskiy

Abstract. The generation of interference patterns of evanescent electromagnetic waves with an essentially sub-wavelength period using dielectric waveguide diffraction gratings is considered. Using simulations within the framework of the electromagnetic theory, the possibility of obtaining high-quality interference patterns due to enhancement of evanescent diffraction orders under resonance conditions is demonstrated. The contrast of the interference patterns in the case of TE polarisation of the incident wave is close to unity. The field intensity in the near-field interference maxima exceeds the intensity of the incident wave by 25–100 times. The possibility of generation of the interference patterns of evanescent waves corresponding to higher diffraction orders is shown. The use of higher orders reduces the requirements to the fabrication technology and allows generation of interference patterns with a high spatial frequency, using diffraction gratings with a low spatial frequency. Examples of generating interference patterns with periods six times smaller than those of the used diffraction gratings are presented.

Keywords: nanolithography, nanophotonics, evanescent wave, interference pattern, diffraction grating.

1. Introduction

Rapid progress of nanotechnology makes it urgent to develop methods for fabricating nanostructures with the feature size of a few tens of nanometres or even a few nanometres. At present one of the basic methods for fabricating nanostructures is the projection photolithography. In this method the minimal achievable size of features is diffraction-limited and equals about a half of the wavelength. One of the ways to improve the resolution in photolithography systems is to reduce the wavelength, i.e., to use short-wave UV or X-ray radiation [1–3]. The

main disadvantages of this approach are complexity and high cost of the used systems. As an alternative to wavelength shortening, different variants of near-field photolithography were proposed, based on the interference patterns of evanescent electromagnetic waves (EEWs) [4–7] or surface electromagnetic waves (SEWs) [8–15]. The use of EEWs and SEWs allows overcoming the diffraction limit and generation of periodic structures with the feature size, by an order of magnitude smaller than the wavelength of the light used.

The authors of paper [4] first demonstrated the possibility of obtaining a one-dimensional interference pattern with EEWs, corresponding to the ± 1 st evanescent orders of a subwavelength diffraction grating. According to the results of simulations within the framework of the electromagnetic theory, the intensity in the maxima of the interference pattern is 3–4 times greater than the intensity of the incident wave, and the pattern period is 2 times smaller than the period of the diffraction grating and is close to a half of the wavelength. The authors of [5–7] proposed the methods of generation of one- and two-dimensional EEW interference patterns under the conditions of total internal reflection of two and four incident waves, respectively. The period of two-dimensional patterns of EEWs in [5–7] is 2–4 times smaller than the incident wavelength. The main disadvantage of the method, proposed in [6, 7], is the use of four beams with a specifically chosen phase and polarisation. The generation of such beams requires a complex optical system.

The authors of [8–14] considered the methods of photolithography based on producing SEW interference patterns. In [8, 9] such a pattern is formed at the surface of a perforated metal film. In [10–12] the SEW interference patterns were obtained using the structures, comprising a diffraction grating and a metal layer coating the substrate. The diffraction grating is intended for the excitation of several SEWs at the lower boundary of the metal film that produce an interference pattern. In [13, 14] similar structures are considered, but instead of a single metal layer a system of metal-dielectric layers is used. The periods of the interference patterns in [8–14] are 2–5 times smaller than the incident wavelength and, thus, are comparable with the periods of interference patterns obtained with EEWs in [5–7].

A distinctive feature of the SEW interference patterns is the much greater factor of field enhancement. In particular, the comparison of SEW interference patterns, formed in the Kretschmann geometry, with the EEW interference patterns, formed under the conditions of total internal

E.A. Bezus, L.L. Doskolovich, N.L. Kazanskiy Institute for Image Processing Systems, Russian Academy of Sciences, ul. Molodogvardeiskaya 151, 443001 Samara, Russia; The State Educational Institution of Higher Professional Education ‘Samara State Aerospace University named after academician S.P. Korolyov’ (National Research University), Moskovskoye sh. 34, 443086 Samara, Russia; e-mail: evgeni.bezus@gmail.com, leonid@smr.ru, kazansky@smr.ru

Received 18 November 2010; revision received 9 February 2011
Kvantovaya Elektronika 41 (8) 759–764 (2011)
Translated by V.L. Derbov

reflection [15], has shown that the intensity of SEW interference patterns is 6–8 times higher and the contrast is by 20%–30% greater than in the EEW interference patterns. In this case the intensity of the electric field in the maxima of the SEW interference pattern at the lower boundary of the metal layer is 30 times greater than the intensity of the incident wave [15].

Moreover, in [11–13] the excitation of SEWs was implemented using higher diffraction orders of the grating with the numbers $\pm n$, $n > 1$. The use of higher orders with the numbers $\pm n$ allows generation of SEW interference patterns with a high spatial frequency using the diffraction gratings with the period $2n$ times greater than that of the interference pattern. This essentially reduces the requirements to the technology of fabricating such structures.

The use of higher diffraction orders for EEW interference pattern generation in dielectric diffraction gratings was thought to be hardly implementable. Indeed, in [11–14] a metal layer or a system of metal-dielectric layers, underlying the grating, play the role of a filter that ‘transmits’ the diffraction orders exciting the SEW, and blocks the other orders. It is the filtering property of the metal layer or the system of metal-dielectric layers that provides the generation of high-contrast SEW interference patterns [10–14].

In the present paper, the possibility of producing high-frequency EEW interference patterns using dielectric diffraction gratings (see Fig. 1), referred to as guided-mode resonant gratings, is investigated. In what follows, we will call these gratings the waveguide diffraction gratings. Waveguide gratings have been intensely studied during the recent ten years as narrow-band spectral filters [16–18]; however, up to now only minor attention has been paid to the study of the field distribution in such systems [19, 20]. In the present paper we demonstrate high efficiency of these structures in the generation of EEW interference patterns.

2. Geometry of the structures and mechanism of interference pattern generation by evanescent electromagnetic waves

The waveguide diffraction gratings considered in this paper are shown in Fig. 1. The gratings are periodic along the x axis; the media below and above them are homogeneous dielectrics. The structures of such types are traditionally used as narrow-band spectral filters that have high reflectance, close to 100%, in the vicinity of definite wavelengths of incident light [17]. This effect is due to resonant excitation of quasi-waveguide eigenmodes in the structure [18].

The reason for using such structures for EEW interference pattern generation is as follows. Under certain conditions, provided by the choice of geometric and physical parameters of the structure, quasi-waveguide modes with the structure resembling that of the modes of a planar waveguide are excited in it [18–20]. The structure shown in Fig. 1a (Structure A) is a binary dielectric diffraction grating, and it may be expected to possess modes that in the near-field region of the grating have the structure, close to a superposition of two evanescent diffraction orders with the numbers $\pm n$. Indeed, at a small relative size of the slits Structure A is close to a planar waveguide, whose permittivity may be evaluated using the methods of the effective medium theory. One can suppose that the structure, shown in Fig. 1b (Structure B), consisting of a binary dielectric

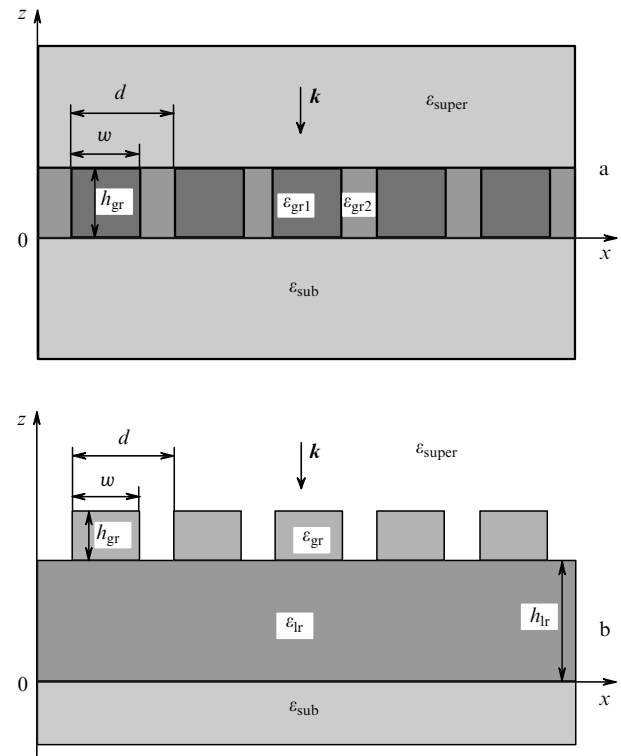


Figure 1. Geometry of the structures.

grating with a waveguide layer may possess modes localised in the waveguiding layer and close to a superposition of two evanescent diffraction orders in the region of substrate.

Under the mode excitation the electric field inside the structure may be essentially enhanced. In particular, according to the results of calculations of the electromagnetic field inside the waveguide gratings [19, 20], the amplitude of the electric field in the maxima of the mode interference patterns inside the grating is 20–40 times greater than the amplitude of the wave, incident on the structure. Hence, under the excitation of modes one should expect also a significant increase in the amplitude of evanescent waves (diffraction orders) in the near field.

The fact that the amplitudes of the evanescent waves can be large under the excitation of modes in periodic structures (diffraction gratings) follows from the description of their properties based on the scattering matrix method [21, 22]. The frequencies of eigenmodes of a periodic structure correspond to poles of the scattering matrix. The complex amplitude of the n th diffraction order in the vicinity of the resonance has the form [23–25]:

$$A_n(\omega) = a_n + \frac{b_n}{\omega - \omega_0}, \quad (1)$$

where ω_0 is the complex frequency of the grating eigenmode; a_n and b_n are slowly varying functions of the real frequency ω of light incident on the structure. For propagating orders the maximal values of the amplitudes are limited by the energy conservation law. The sum of intensities of the propagating orders in the gratings made of a nonabsorbing material is equal to unity. Large amplitudes of evanescent orders do not contradict the energy conservation law and, according to Eqn (1), at $\text{Im}(\omega_0) \ll 1$ (i.e., at high quality factor of the mode [24])

in the near field can be much greater than the amplitude of the incident wave.

In the general case the field in the region of the substrate is presented as a superposition of an infinite number of transmitted diffraction orders (propagating and evanescent). However, due to the effect of field enhancement under the excitation of modes [19, 20] in the near field one can expect the formation of a dominant distribution with the structure close to a superposition of two modes, corresponding to evanescent diffraction orders.

Let us write down the expressions for the field intensity (square modulus of the electric field strength), corresponding to the superposition of $\pm n$ th orders. In the case of TE polarisation the electric and magnetic fields of the n th transmitted diffraction order have the form:

$$\mathbf{E}_n = (0, E_y, 0) = (0, A_n^{\text{TE}}/2, 0) \exp[i(k_{x_n}x - k_{z_n}z)],$$

$$\mathbf{H}_n = (H_x, 0, H_z) = (k_{z_n}, 0, k_{x_n})E_y/k_0,$$

where $k_{x_n} = 2\pi n/d$ is the propagation constant of the n th diffraction order; d is the period of the grating; $k_{z_n} = i(k_{x_n}^2 - k_0^2 \epsilon_{\text{sub}})^{1/2}$; ϵ_{sub} is the permittivity of the substrate; A_n^{TE} is the complex amplitude of the mode of the n th order. Note, that in this notation for k_{z_n} the decay of the orders $\pm n$ in the substrate is taken into account (at $z \leq 0$). For symmetric structures, considered in the paper, the complex amplitudes of the orders with the numbers $\pm n$ are equal in modulus and can be presented as

$$A_n^{\text{TE}} = A_{\pm n}^{\text{TE}} \exp(i\varphi), \quad A_{-n}^{\text{TE}} = A_{\pm n}^{\text{TE}} \exp(-i\varphi),$$

where $A_{\pm n}^{\text{TE}}$ is a certain complex constant; $\varphi \in [0, 2\pi)$. The corresponding intensity in the region of the substrate in this case will have the form

$$I_{\pm n}^{\text{TE}}(x, z) = |A_{\pm n}^{\text{TE}}|^2 \cos^2(k_{x_n}x + \varphi) |\exp(-ik_{z_n}z)|^2. \quad (2)$$

For TM polarisation of the incident wave the magnetic and electric fields of the n th transmitted diffraction order may be written as

$$\mathbf{H}_n = (0, H_y, 0) = (0, A_n^{\text{TM}}/2, 0) \exp[i(k_{x_n}x - k_{z_n}z)],$$

$$\mathbf{E}_n = -(k_{z_n}, 0, k_{x_n})H_y/(k_0 \epsilon_{\text{sub}}).$$

In this case, with the expression for k_{z_n} taken into account, the intensity of the field will have the form

$$I_{\pm n}^{\text{TM}}(x, z) = \frac{|A_{\pm n}^{\text{TM}}|^2}{2k_0^2 \epsilon_{\text{sub}}^2} [2k_{x_n}^2 - k_0^2 \epsilon_{\text{sub}} - \cos(2k_{x_n}x + 2\varphi)k_0^2 \epsilon_{\text{sub}}] |\exp(-ik_{z_n}z)|^2. \quad (3)$$

According to Eqns (2), (3), the period of the interference pattern of the modes with the orders $\pm n$ is given by the expression

$$d_{\text{ip},n} = \pi/k_{x_n} = d/2n. \quad (4)$$

It is interesting to note, that at TE polarisation the contrast of the interference pattern (2) is equal to unity. For the case of TM polarisation the contrast is easily derived from Eqn (3) that yields

$$K_{\text{TM},n} = \frac{\epsilon_{\text{sub}}}{2(k_{x_n}/k_0)^2 - \epsilon_{\text{sub}}}. \quad (5)$$

It follows from Eqn (5) that with increasing k_{x_n} (which means the decrease in the period of the interference pattern) the contrast of the produced interference pattern decreases.

Note, that in the diffraction gratings shown in Fig. 1 the modes of complex configuration may exist that essentially differ in field distribution from those of a planar waveguide. For such modes the EEW interference pattern will also have complex form. Complex interference patterns are of less interest for practical applications in the field of interference lithography; that is why in this paper the consideration is restricted to the interference patterns, described by Eqns (2) and (3).

3. Results of simulations and discussion

The possibility of producing the EEW interference patterns (2), (3) was studied in the case of a normally incident plane wave with $\lambda = 453$ nm (corresponding to a InGaN/GaN heterostructure laser) for Structure A and with $\lambda = 441.6$ nm (corresponding to a helium-cadmium laser) for Structure B. Note, that the indicated wavelengths lie in the range used in the near-field interference lithography [4, 8, 10, 15]. The following permittivities of the materials were used [26]: $\epsilon_{\text{super}} = 2.15$ (SiO₂), $\epsilon_{\text{gr1}} = 4.41$ (ZnO), $\epsilon_{\text{gr2}} = \epsilon_{\text{sub}} = 2.56$ for Structure A and $\epsilon_{\text{super}} = 1$, $\epsilon_{\text{gr}} = \epsilon_{\text{lr}} = 4.41$, $\epsilon_{\text{sub}} = 2.56$ for Structure B (see Fig. 1). Note, that $\epsilon_{\text{sub}} = 2.56$ corresponds to standard photoresists.

To model the light diffraction by the structures and to calculate the interference pattern intensity, Maxwell's equations were solved numerically using the rigorous coupled-wave analysis [27–29], aimed at simulating light diffraction by periodic structures. In the case of binary gratings the only approximation is made within this method, namely, the permittivity function for the grating material is approximated by a truncated Fourier series. In the framework of the method the electric field below and above the structure is taken to be a superposition of plane waves (diffraction orders). Inside the structure the electromagnetic field is represented as an expansion in Fourier modes [27, 28], the calculation of which is reduced to an eigenvalue problem. Successively imposing the conditions of equality of tangential components of the electromagnetic field at the boundaries of the structure [the interface between the upper medium and the grating, the interface between the grating and the layer (for Structure B) and the interface between the structure and the substrate] reduces the determination of the amplitudes of transmitted and reflected diffraction orders to the solution of a system of linear equations [27, 28].

The geometric parameters of the structures under study were determined as a result of optimising the criterion

$$g(\mathbf{p}) = \frac{1}{\max_x \{I_{\pm n}(x; \mathbf{p})\}} \times \int_0^d \left(\frac{I(x; \mathbf{p}) - I_{\pm n}(x; \mathbf{p})}{\max_t \{I_{\pm n}(t; \mathbf{p})\}} \right)^2 dx \rightarrow \min, \quad (6)$$

where \mathbf{p} is the vector of geometric parameters [$\mathbf{p} = (w, h_{\text{gr}})$ for Structure A and $\mathbf{p} = (w, h_{\text{gr}}, h_{\text{lr}})$ for Structure B]; $I(x; \mathbf{p})$ is the calculated intensity, formed by the structure at the

interface between the structure and the substrate (at $z = 0$); $I_{\pm n}(x; \mathbf{p})$ is the intensity of the interference pattern of the $\pm n$ th diffraction order at $z = 0$, defined by Eqns (2), (3). The first factor in Eqn (6) is responsible for maximising the field intensity at the peaks of the interference pattern, the second factor is a measure of similarity of the calculated interference pattern to that produced by the interference of the $\pm n$ th diffraction order modes.

It should be noted that the generation of EEW interference patterns is of particular interest when $n > 1$. In this case the period of the EEW interference pattern (4) will be $2n$ times smaller than the period of the grating. Thus, the use of higher orders reduces the requirements to the technologic implementation of the structure and allows generation of high-frequency EEW interference patterns by means of diffraction structures with a low spatial frequency.

The study of possibility to form EEW interference patterns using Structure A were performed at $n = \pm 3$, the period of grating being $d = 750$ nm and the incident wave being TM-polarised. In this case the period of the resulting interference pattern is $d_{ip3} = d/6 = 125$ nm, which corresponds to the feature size of nearly 60 nm (more than 7 times smaller than the wavelength of the incident light). The geometric parameters of the structure $h_{gr} = 141$ nm and $w = 675$ nm were found as a result of optimisation of criterion (6). Figure 2a presents the distribution of the electric field in the calculated structure that demonstrates generation of a quasi-waveguide mode [19, 20]. The interference patterns in the region of the substrate at different distances from the interface between the grating and the substrate (photoresist) are shown in Fig. 2b. The quantities in Fig. 2 and in other figures are normalised to the intensity $|E_0|^2$ of the wave incident on the structure. The intensity of the interference maxima at the interface is more than 100 times greater than that of the incident wave, which is comparable with the results of [11,12] on plasmonic interference lithography. The main contribution to the near field is provided by the evanescent orders with the numbers ± 3 . According to the calculations, their amplitudes are more than 6 times greater than the amplitude of the zero diffraction order and more than 20 times greater than the amplitudes of other transmitted orders. The contrast of the interference pattern at the interface is 0.68, which is close to the theoretical estimate (0.64), obtained from Eqn (5). When moving off the boundary, the contrast is reduced, and at the distance of 100 nm it is about 0.54. The reduction of the contrast is associated with the presence of propagating diffraction orders in the transmitted field, whose total intensity amounts to 0.76. At the distance 160 nm the contrast is reduced to 0.2. This value is minimal necessary to record the interference pattern using standard photoresists [30].

The study of possibility to produce EEW interference patterns using Structure B was carried out at $d = 720$ nm, $n = \pm 3$ and a TE-polarised incident wave. The period of the formed interference pattern is $d_{ip3} = d/6 = 120$ nm, which corresponds to the feature size of 60 nm. The geometric parameters of the structure ($h_{gr} = 155$ nm, $h_r = 763$ nm, $w = 349$ nm) were also found as a result of optimising criterion (6). Figure 3a shows the distribution of the electric field in the structure. The intensity of the interference patterns below the structure at different distances from the interface between the waveguide layer and the photoresist is presented in Fig. 3b. The intensity in the

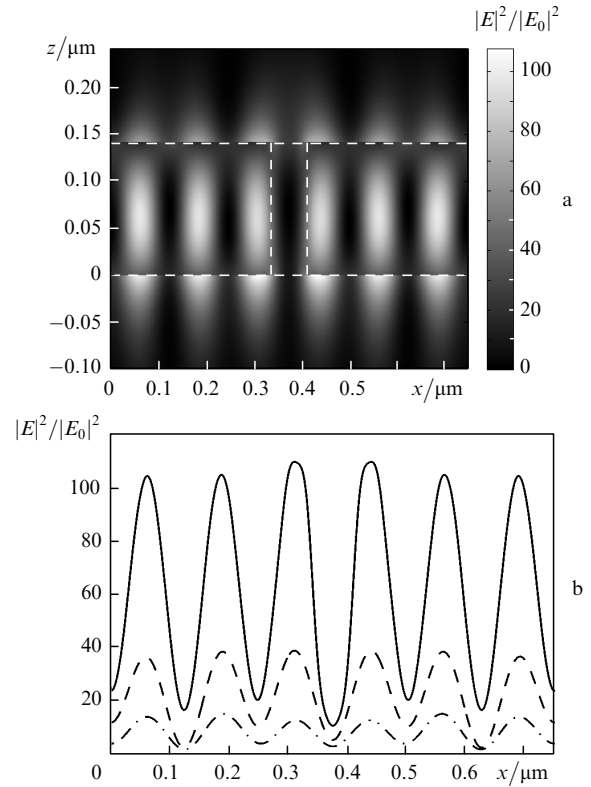


Figure 2. Distribution of the electric field in Structure A under the normal incidence of a TM-polarised wave (one period of the grating shown by a dashed line) (a) and the interference pattern at different distances from the interface between the grating and substrate (one period of grating) (0 nm – solid line, 50 nm – dashed line, 100 nm – dash-and-dot line) (b). The structure parameters are: the grating height 141 nm, the step width 675 nm; the mode is excited by the grating orders with the numbers ± 3 .

interference maxima at the lower boundary is more than 25 times greater than the intensity of the incident wave, and the contrast amounts to 0.99, which also agrees with the theoretical estimate. As in the previous example, the major contribution into the near field is provided by the evanescent orders with the numbers $n = \pm 3$ the amplitudes of which are 9 times greater than the amplitude of the zero diffraction order and more than 19 times greater than the amplitudes of the rest transmitted orders. Note, that such high values of the mode amplitudes of the orders $n = \pm 3$ are obtained under the resonance conditions, i.e., under the excitation of the quasi-waveguide mode in the structure (Fig. 3a). Off the interface the contrast decreases and at the distance 130 nm equals 0.2.

The waveguide gratings were also calculated for the case of producing interference patterns of the orders ± 1 and ± 5 . The calculation was performed using the minimisation of Eqn (6) with the parameter values specified above. For $n = \pm 1$ we managed to reduce the transmission (the intensity of the zero transmitted order) to 0.01. In this case the contrast of the interference pattern, in fact, does not depend on the distance from the interface. For TE polarisation of the incident wave the value of the contrast remains high (greater than 0.99) over the entire depth of the interference pattern decay. On the contrary, for $n = \pm 5$ the total intensity of the propagating transmitted orders increases, which leads to a faster decrease in the contrast as

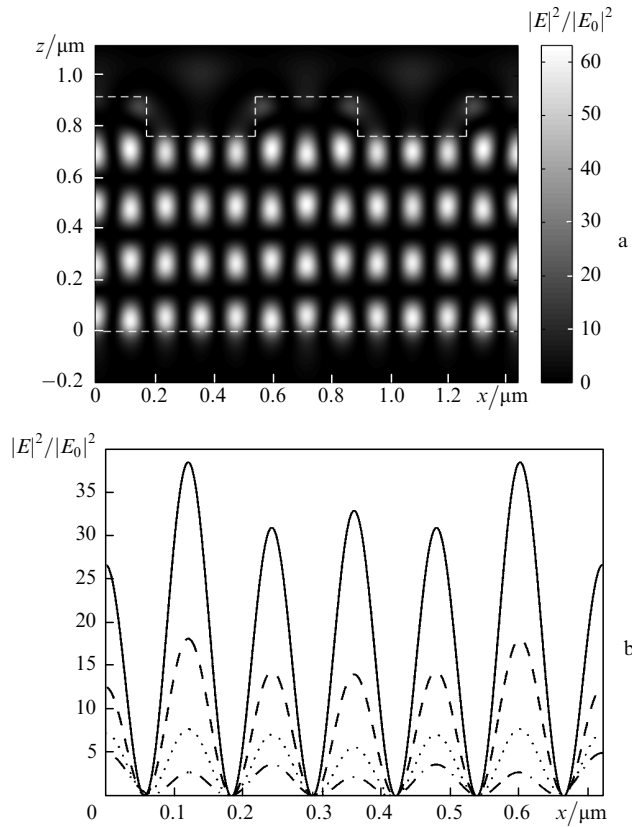


Figure 3. Distribution of the electric field in Structure B under the normal incidence of a TE-polarised wave (two periods of the grating, shown by white dashed line) (a) and the interference pattern at different distances from the interface between the waveguide layer and the substrate (one period of the grating) (0 nm – solid line, 60 nm – dashed line, 90 nm – dash-and-dot line) (b). The structure parameters are: the height of the grating 155 nm, the layer thickness 763 nm, the step width 349 nm; the mode is excited by the grating orders with the numbers ± 3 .

compared to Figs 2, 3. The contrast value at $n = 5$ becomes smaller than 0.2 already at the distance of 40–50 nm from the interface.

The proposed approach may be generalised over the case of generation of two-dimensional EEW interference patterns. In this case a three-dimensional diffraction grating is used (Fig. 4a), the parameters of which are calculated from the condition of interference pattern generation by the orders with the numbers $(\pm n, 0)$, $(0, \pm n)$ at the bottom of the structure, based on optimising the criterion, analogous to Eqn (6). As an example of producing a two-dimensional interference pattern at $n = 3$, a diffraction structure was calculated with the period $d_x = d_y = 660$ nm, $\lambda = 441.6$ nm, and material parameters $\epsilon_{\text{super}} = 1.69$, $\epsilon_{\text{sub}} = 2.56$, $\epsilon_{\text{gr}} = \epsilon_{\text{lr}} = 4.41$. The geometric parameters of the structure, calculated as a result of the optimisation procedure, are the following: $h_{\text{gr}} = 287$ nm, $h_{\text{lr}} = 305$ nm, $w_x = w_y = 200$ nm. Note that the configuration of the resulting EEW interference patterns depends on the polarisation of the incident wave. Figure 4b shows the interference pattern at the interface between the waveguide layer and the photoresist, produced by the incident wave with the mixed linear polarisation. In this case the interference pattern is rotated by the angle 45° with respect to the coordinate axes and its period is $d_{\text{ip}} = d/(3\sqrt{2}) = 155$ nm. A similar structure is demonstrated by the SEW interference

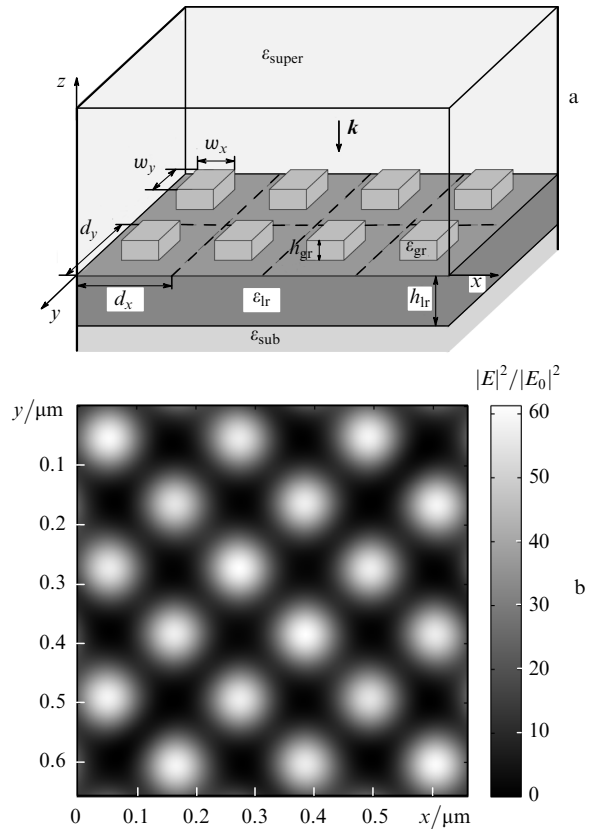


Figure 4. Diffraction structure for generation of two-dimensional EEW interference patterns (a) and two-dimensional interference pattern at the interface between the waveguide layer and the substrate (one period of the grating) (b). The structure parameters are: the height of the grating 287 nm, the layer thickness 305 nm, the step width 200 nm; the mode is excited by the grating orders with the numbers $(\pm 3, 0)$, $(0, \pm 3)$.

patterns in [12]. The intensity of interference peaks in Fig. 4b is more than 50 times greater than that of the incident wave, and the contrast of the pattern is close to unity.

4. Conclusions

Based on the numerical simulations in the framework of the rigorous electromagnetic theory the possibility of generation of EEW interference patterns using waveguide diffraction gratings is demonstrated. For the incident light wavelengths considered in the paper, the period of the EEW interference patterns amounts to 120–125 nm, which corresponds to the feature size of about 60 nm ($\sim \lambda/7$). The contrast of the interference patterns, produced by the TE-polarised incident wave, is close to unity, while the intensity of the interference peaks in the near field is more than 25 times greater than that of the incident wave. The possibility of generation of one- and two-dimensional interference patterns, corresponding to higher evanescent diffraction orders, is demonstrated. The use of higher orders reduces the requirements to the technology of the grating fabrication and allows generation of patterns with high spatial frequency using the diffraction surface relief having a low spatial frequency.

The proposed approach may be applied to the fabrication of periodic structures with nanoscale features using the method of contact photolithography.

Acknowledgements. The work was supported by the Russian Foundation for Basic Research (Grant Nos 10-02-01391, 10-07-00553, and 11-07-00153, 11-07-12036), by the Presidential Grant for Support of Leading Scientific Schools (Grant No. NSH-7414.2010.9) and by the Russian–American Program ‘Basic Research and Higher Education’ (CRDF Grant PG08-014-1).

References

1. Bates A.K., Rothschild M., Bloomstein T.M., Fedynshyn T.H., Kunz R.R., Liberman V., Switkes M. *IBM J. Res. Dev.*, **45**, 605 (2001).
2. Gwyn C.W., Stulen R., Sweeney D., Attwood D. *J. Vac. Sci. Technol. B*, **16**, 3142 (1998).
3. Silverman J.P. *J. Vac. Sci. Technol. B*, **16**, 3137 (1998).
4. Blaikie R.J., McNab S.J. *Appl. Opt.*, **40**, 1692 (2001).
5. Martinez-Anton J.C. *J. Opt. A.: Pure Appl. Opt.*, **8**, 213 (2006).
6. Chua J.K., Murukeshan V.M., Tan S.K., Lin Q.Y. *Opt. Express*, **15**, 3437 (2007).
7. Murukeshan V.M., Chua J.K., Tan S.K., Lin Q.Y. *Opt. Express*, **16**, 13857 (2008).
8. Luo X., Ishihara T. *Appl. Phys. Lett.*, **84**, 4780 (2004).
9. Srituravanich W., Fang N., Sun C., Luo Q., Zhang X. *Nano Lett.*, **4**, 1085 (2004).
10. Jiao X., Wang P., Zhang D., Tang L., Xie J., Ming H. *Opt. Express*, **14**, 4850 (2006).
11. Bezus E.A., Bykov D.A., Doskolovich L.L., Kadomin I.I. *J. Opt. A: Pure Appl. Opt.*, **10**, 095204 (2008).
12. Bezus E.A., Doskolovich L.L. *Opt. Commun.*, **283**, 2020 (2010).
13. Xiong Y., Liu Z., Zhang X. *Appl. Phys. Lett.*, **93**, 111116 (2008).
14. Yang X., Zeng B., Wang C., Luo X. *Opt. Express*, **17**, 21560 (2009).
15. Guo X., Du J., Guo Y., Yao J. *Opt. Lett.*, **31**, 2613 (2006).
16. Brundrett D.L., Glytsis E.N., Gaylord T.K., Bendickson J.M. *J. Opt. Soc. Am. A*, **17**, 1221 (2000).
17. Magnusson R., Shin D., Liu Z.S. *Opt. Lett.*, **23**, 612 (1998).
18. Tamir T., Zhang S. *J. Opt. Soc. Am. A*, **14**, 1607 (1997).
19. Wei C., Liu S., Deng D., Shen J., Shao J., Fan Z. *Opt. Lett.*, **31**, 1223 (2006).
20. Sun T., Ma J., Wang J., Jin Y., He H., Shao J., Fan Z. *J. Opt. A: Pure Appl. Opt.*, **10**, 125003 (2008).
21. Gippius N.A., Tikhodeev S.G. *Usp. Fiz. Nauk.*, **179**, 1027 (2009) [*Phys. Usp.*, **52**, 967 (2009)].
22. Sarrazin M., Vigneron J.-P., Vigoureux J.-M. *Phys. Rev. B*, **67**, 085415 (2003).
23. Gippius N.A., Tikhodeev S.G., Ishihara T. *Phys. Rev. B*, **72**, 045138 (2005).
24. Belotelov V.I., Bykov D.A., Doskolovich L.L., Kalish A.N., Zvezdin A.K. *Zh. Eksp. Teor. Fiz.*, **137**, 932 (2010). [*J. Exp. Theor. Phys.*, **110** (5), 816 (2010)].
25. Bykov D.A., Doskolovich L.L., Soifer V.A., Kazanskiy N.L. *Zh. Eksp. Teor. Fiz.*, **138**, 1093 (2010). [*J. Exp. Theor. Phys.*, **111** (6), 967 (2010)].
26. Bass M. *Handbook of Optics* (New York: McGraw-Hill, 1995) Vol. II.
27. Moharam M.G., Pommet D.A., Grann E.B., Gaylord T.K. *J. Opt. Soc. Am. A*, **12**, 1077 (1995).
28. Moharam M.G., Grann E.B., Pommet D.A., Gaylord T.K. *J. Opt. Soc. Am. A*, **12**, 1068 (1995).
29. Li L. *J. Opt. Soc. Am. A*, **13**, 1870 (1996).
30. Madou M.J. *Fundamentals of Microfabrication* (Boca Raton: CRC Press, 2002).